Protein Engineering vol.6 no.6 pp.565–574, 1993

An NMR study on the DNA-binding SPKK motif and a model for its interaction with DNA

Masashi Suzuki[1], Mark Gerstein and Tony Johnson

MRC Laboratory of Molecular Biology, Hills Road, Cambridge CB2 2QH, UK

[1]To whom correspondence should be addressed

The solution structure of one and two repeats of the 'SPKK' DNA-binding motif is reported on the basis of NMR measurements. In dimethylsulphoxide (DMSO) the major population (approximately 90%) of peptides, SPRKSPRK(S2) and GSPKKSPRK(S2b), adopts a conformation, which has two *trans* prolines. The two 'SP(R/K)K' units in these peptides are equivalent and each adopts a turn structure exchanging with an extended structure. This is suggested by an NOE connectivity of the β-turn type, between the backbone amide protons of residues (*i*+2) and (*i*+3) and NOE connectivities of the Asx(σ)-turn type, between protons of the *i*th Ser and the backbone amide proton on residue (*i*+2). This suggests that each SP(R/K)K unit has a structural intermediate between (or a combination of) a β-turn and an Asx(σ)-turn. In 90–10% DMSO/H_2O at 4°C the two units of S2 are connected more tightly by folding into a short 3_{10} helix, broken at the second proline. For another peptide, Thr–Pro–Arg–Lys(T1), the major population (75%) in 100% DMSO comprises a β-turn in rapid exchange with an extended structure. We did not observe an NOE connectivity of the Asx(σ) type with the T1 peptide. A possible structure of the SPKK motif in the complex with DNA is discussed.

Key words: Asx-turn/β-turn/DNA-binding/NMR/SPKK motif

Introduction

One of the most important subjects in protein structure studies today is to reveal how proteins recognize features of DNA. In 1989 one of us proposed a novel DNA-binding unit, the 'SPKK' motif, which has the (Ser/Thr)–Pro–(Lys/Arg)–(Lys/Arg) sequence (Suzuki, 1989). Since then, the DNA binding of the SPKK motif has been studied using synthetic peptides (Churchill and Suzuki, 1989; Suzuki, 1989; Erard *et al.*, 1990; Reeves and Nissen, 1990). It has been proved that the SPKK motif binds into the minor groove of DNA at A–T-rich sequences (Churchill and Suzuki, 1989).

One of us has proposed that the SPKK motif folds into a turn structure which is stabilized by two possible hydrogen bonds, the β-turn type, between the CO of residue (*i*) and NH of residue (*i*+3) or the Asx(σ) type using the side chain oxygen of (Ser/Thr) and the NH of residue (*i*+2) (Suzuki, 1989). A statistical study has shown that more than 40% of the (S/T)PXX sequences in protein crystal structures fold into a type (I) β-turn or one of a few closely related turn structures and that many such type (I) β-turns have additional hydrogen bond(s), one between NH of the (*i*+2) residue and the side chain oxygen of (Ser/Thr) (the σ-turn type) and/or the other between NH of the (*i*+3) residue and the side chain oxygen of Thr (the γ-turn type) (Suzuki and Yagi, 1991). However, the structure of the SPKK motif in solution remained unknown.

The purpose of this paper is to examine the structure of the SPKK motif in solution by NMR and to discuss the structure of the motif in the complex with DNA. In this study three synthetic peptides, H–Thr–Pro–Arg–Lys–OH (T1), H–Ser–Pro–Arg–Lys–Ser–Pro–Arg–Lys–OH (S2) and H–Gly–Ser–Pro–Lys–Lys–Ser–Pro–Arg–Lys–$CONH_2$ (S2b), were used.

The T1 peptide constitutes one unit of the motif. The N-terminal residue is Thr rather than Ser and it is closely related to the sequences of DNA-binding proteins, TPKK in the C-terminus of histone H1, TPKR in HMG I and TPAKK in nucleolin (Lapeyer *et al.*, 1987; Lund *et al.*, 1987; Erard *et al.*, 1990; and see also a review, Suzuki, 1991). The T1 peptide itself is a hormone, kentsin (Kent, 1975). It is unlikely that it penetrates the cell nucleus and binds to DNA *in vivo* but DNA binding of this peptide *in vitro* (Reeves and Nissen, 1990; Suzuki, unpublished results) in addition to that of S2 (Churchill and Suzuki, 1989) has been proved.

The peptides, S2 and S2b, were chosen to investigate the motifs starting with Ser and the connection between two such motifs; in the N-terminal region of sea urchin histone H1, six SP(R/K)(R/K) sequences are found and four of them are adjacent (Suzuki, 1989 and references therein). S2 was designed to mimic a combination of basic residues in T1, while chemically blocking both termini in S2b was intended to increase the stability of its structure. It may have done so but in the event we chose to work with S2 in preference to S2b, because the almost exact degeneracy of many corresponding signals from the two units in S2b severely complicated assignment.

Materials and methods

NMR measurements

The S2 and S2b peptides were synthesized by solid phase methods. The T1 peptide was purchased from Sigma. S2b was purified by HPLC. S2 and T1 were sufficiently pure that further purification was not necessary.

The three peptides were dissolved in either 100% [$^2H_6$]dimethylsulphoxide (DMSO) or 90% [$^2H_6$]dimethylsulphoxide–10% H_2O to yield 10 mM solutions (10 mg/ml for S2 and S2b, 5 mg/ml for T1). Three sets of [^{1}H]NMR spectra were recorded with S2 or S2b using a Bruker AMX500 spectrometer; those of S2 in a 90–10% DMSO/H_2O mixture at 4°C, those of S2 in 100% d_6-DMSO at 27°C and those of S2b in 100% d_6-DMSO at 27°C. The data collected comprised the following: ^{1}H 1-D spectra and double-quantum filtered (DQF) COSY, TOCSY, NOESY and ROESY spectra. For the T1 peptide ^{13}C 1-D and (^{13}C, ^{1}H) heteronuclear multiple coherence (HMQC) long-range shift correlation spectra were also recorded.

2-D spectra were acquired using time-proportional phase incrementation (TPPI) in t_1 to achieve F_1 quadrature detection (Bodenhausen *et al.*, 1980; Marion and Wüthrich, 1983). True quadrature was employed in t_2, with simultaneous acquisition of complex data points. The spectral width in both dimensions was 8 kHz, the filter width was 12 kHz, and the data size was 1 K

(complex) × 512 (real) in the time domain and 2 K (complex) × 512 (complex) in the frequency domain.

The HMQC spectra were acquired without decoupling of ^{13}C during t_2 and with the Δ_1 delay set to 50 ms to optimize the experiment for detection of long-range (^{13}C, ^{1}H) connectivities. The F_2 parameters used were identical to those for the homonuclear experiments, while in F_1 the spectral width was limited to the carbonyl region by employing a selective 90° pulse (128 step Gaussian, truncated at 5%, 860 μs duration) as the first ^{13}C pulse. The F_1 spectral width was 1.5 kHz, 64 increments were acquired and the frequency domain size was 128 points.

In all experiments, water suppression was achieved using presaturation during the relaxation delay (2 s) (and during the mixing time in the case of NOESY), using an irradiation field of the same frequency as the phase coherent with the ^{1}H hard pulses (Zuiderweg *et al.*, 1986). The mixing times chosen were as follows: NOESY experiments, 150 ms for S2 and S2b, 300 ms for T1, ROESY experiments, 100 ms for S2 and S2b, 200 ms for T1 and TOCSY experiments, 46 ms for S2 and S2b, 76 ms for T1. The spin-locking field strength ($\gamma B_1/2\pi$) for the ROESY and TOCSY experiments was approximately 5 kHz. TOCSY experiments employed the DIPSI-2 mixing sequence (Shaka *et al.*, 1988) to achieve minimal phase distortion with two z-filters flanking the spin-locking period (Rance, 1987).

During data processing, time-domain data were multiplied in both dimensions by a sine-bell window phase shifted through $\pi/8$ radians and the phase of the 2-D spectrum was adjusted to double-absorption. For in-phase spectra (NOESY and TOCSY), F_2 baseline errors were corrected by applying an automatic polynomial baseline correction of maximum order 1. Spectra were referenced relative to the [$^{2}H_5$]dimethylsulphoxide signal at 2.49 p.p.m.

Model building study

Models were built using the program CHARMM (version 2.1, Brooks *et al.*, 1983) and XPLOR (version 2.2, Brunger *et al.*, 1987), displayed using INSIGHT (Dayringer *et al.*, 1986) and FRODO (Jones, 1982) and plotted with INSIGHT (Dayringer *et al.*, 1986) and ARTPLOT (Lesk and Hardmann, 1982). The coordinates of the netropsin–DNA complex (Kopka *et al.*, 1985) are taken from the Protein Data Bank (Bernstein *et al.*, 1977).

Here the convention will be adopted that the Ser/Thr in each (S/T)P(R/K)K unit will always be referred to as position (*i*), the Pro will be referred to as position (*i*+1) and so on.

Results and discussion

General features of the NMR spectra

Assignment of the NMR spectra of each peptide was carried out using scalar coupling connectivities detected in DQF COSY spectra and TOCSY spectra and sequential connectivities detected in NOESY spectra (Wüthrich, 1986) (Figures 1–5). All NOE cross-peaks have the same sign as the diagonal, i.e. the molecules are within the negative NOE regime. Cross-peaks due to conformational exchanges were distinguished from those due to NOE interactions using their relative signs in ROESY spectra, although only relatively strong NOE interactions gave rise to appreciable cross-peak intensity in ROESY.

NMR spectra of the three peptides are complicated by *trans–cis* isomerism of Pro, which occurs slowly on the NMR time-scale and results in the observation of two or more sets of signals (Figures 1–5). The major population possesses *trans* X–Pro connectivities. Similar isomerism has been reported with many other Pro-containing small peptides (see, for example, Dyson *et al.*, 1985). NMR spectra of S2 and S2b show that the structural features of the two peptides are similar and are not affected greatly by the difference in the solvent. The structures of the first and the second SP(R/K)K units in each peptide are also similar.

Trans–cis isomerism of Pro

Evidence that the Thr–Pro link in the major (M) conformation (approximately 75%) of T1 is *trans*, while that in the minor (m) conformation (approximately 25%) is *cis*, is provided by NOE connectivities. For a *trans* X–Pro linkage, the H_α proton of X is much closer to the H_δ protons of Pro than to the H_α proton of Pro, whereas for a *cis* X–Pro linkage the H_α proton of X is much closer to the Pro H_α proton than to either of the Pro H_δ protons (Wüthrich *et al.*, 1984). For the M conformation of T1, a relatively strong NOE connectivity between the Pro H_δ and Thr H_α resonances was observed (labelled 3 in Figure 1), but for the m conformation an NOE connectivity between the Pro H_α and Thr H_α resonances was observed (labelled 13 in Figure 1). Moreover, the ^{13}C shifts for Pro C_α and C_δ were consistent with this assignment, those of the M conformation being 'inside' those of the m conformation [i.e. these ^{13}C shifts were in the order $C_\delta(m) < C_\delta(M) < C_\alpha(M) < C_\alpha(m)$]. This so-called back-to-back character is expected for the *trans–cis* isomerism of an X–Pro linkage and arises due to the different influences of the magnetic anisotropy of the carbonyl group of X in the two conformations (Wüthrich, 1976). Exchange cross-peaks between proton resonances of the M and m conformations were observed for the NH signals of Arg and Lys and the H_α signals of Thr, Pro and Arg, in a NOESY spectrum (Figure 1). The ratio of the M conformation to the m conformation is independent of peptide concentration within the range 0.5–5 mg/ml.

A similar analysis of NOE connectivities shows that the two Ser–Pro links in the major (M) conformation of S2 and S2b are *trans*, while the two Ser–Pro links in the minor (m) conformation are *cis*; the ratio of M to m is approximately 10:1. Exchange cross-peaks between some proton resonances of the M and m conformations were observed; NH signals of Arg3, Ser5 and Arg7 and the H_α signals of Pro2, Ser5 and Pro6 in a NOESY spectrum of S2 in 100% DMSO and the NH signals of Ser2, Lys4, Ser6 and Arg8 and the H_α signals of Ser2, Pro3 and Pro7 in a NOESY spectrum of S2b in 100% DMSO. In a NOESY spectrum of S2 in 90% DMSO at 4°C, exchange cross-peaks were not observed.

Two more combinations of Pro conformations are possible for S2 and S2b, *trans* for the first Pro and *cis* for the second and *cis* for the first and *trans* for the second. In the NOESY spectra, we observed cross-peaks corresponding to an additional Lys–Ser connectivity, which was not assigned to the M or m conformations. The chemical shift of the Ser H_α proton in this third conformation is very similar to that in the M conformation, perhaps suggesting that the third conformation has *trans* Pro in the second unit and *cis* in the first. The NOESY spectrum of S2 in 100% DMSO shows further NOE connectivities which may belong to third or fourth conformations.

A trace amount of a third conformation of T1 was also observed and was found to be in slow exchange with the m conformation (but not detectably with M; see exchange peaks [301]–[304] in Figure 1). As might be expected from its exchange with m rather than M, this third conformation has a *cis* Thr–Pro peptide link, as we observed an NOE connectivity between Thr H_α and Pro H_α. However, we do not know the

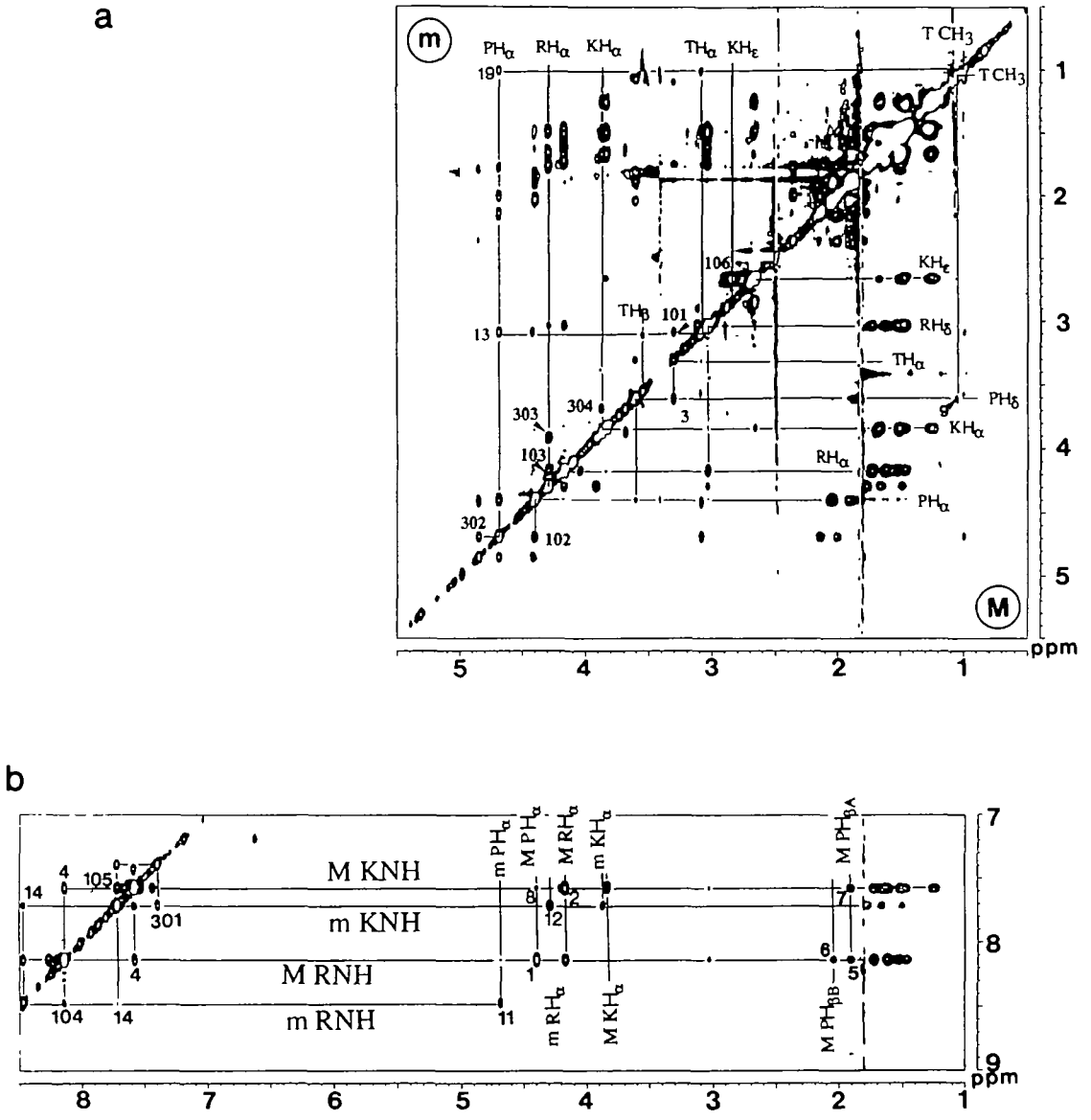

Fig. 1. Two portions of a NOESY spectrum of the T1 peptide in 100% DMSO. Resonances of the major (M) and minor (m) conformations are indicated. Cross-peaks are numbered as follows: NOE connectivities for the M conformation, P H_α–R NH(S)* [1], R H_α–K NH(S)* [2], T H_α–P H_δ(S)* [3], R NH–K NH(S)* [4], P $H_{\beta A}$–R NH(S)* [5], P $H_{\beta B}$–R NH(S)* [6], P $H_{\beta A}$–K NH(w)* [7], P H_α–K NH(w) [8], T $C_\gamma H_3$–P H_δ(w)* [9]; NOE connectivities for the m conformation, P H_α–R NH* [11], R H_α–K NH* [12], T H_α–P H_α [13], R NH–K NH [14], T $C_\gamma H_3$–P H_α [19]; exchange connectivities between M and m, T H_α [101], P H_α* [102], R H_α [103], R NH [104], K NH [105], K H_ε* [106]. Signals confirmed as a genuine direct NOE interaction or an exchange connectivity, using their relative signs in ROESY, are marked (*). Intensities are indicated as strong (S) or weak (w). Cross-peaks, [301]–[304], result from exchange between the m conformation and a third conformation (see text). In (a), assignments for the M conformation are indicated in the lower right triangle, while those for the m conformation are indicated in the upper left triangle.

nature of the third conformation or the mechanism of its slow exchange with the m conformation.

Turn structure of the major conformation

The major conformation (M) will be discussed first. In the NOESY spectra of the three peptides, each backbone amide proton shows a stronger NOE cross-peak to the H_α proton of the sequentially preceding residue than to its own (Figures 1 and 3), as would be expected for an extended conformation. However, other NOE connectivities are observed that are characteristic of a turn conformation; in T1, there is an NH(i+2)–NH(i+3) NOE connectivity (Figure 5a), characteristic of a β-turn (Wüthrich *et al.*, 1984) and NOE connectivities between Ser(i) and NH(i+2) which were observed for many SP(R/K) units (Figure 5a), may indicate a hydrogen bond between the OH of Ser and the backbone amide of residue (i+2), as we will discuss later in this paper [Figure 6b and see also Figure 1 of Suzuki and Yagi (1991)]. Thus, it appears that the major conformation of each peptide is itself in fast exchange between extended and more structured states, as has been observed for many other short peptides (see, for example, Dyson *et al.*, 1985). In what follows, we consider the nature of the structured state.

The peptides, T1 and S2, show NMR properties consistent with a β-turn structure. For such a turn, NOE connectivities are expected between the NH of residue (i+2) and the NH of residue (i+3) [shown as A in Figure 6; Wüthrich *et al.* (1984)] and, more weakly, between H_α of residue (i+1) (here Pro) and the NH of residue (i+3) [shown as B in Figure 6; Wüthrich *et al.*

	NH	$C_\alpha H$	$C_\beta H$		$C_\gamma H$		$C_\delta H$	$C_\epsilon H$
			A	B	A	B		
^{1}Thr(M)	--	3.31	3.54	---	1.06		---	
^{2}Pro(M)	--	4.41	2.04	1.90	1.89	1.82	3.60	
^{3}Arg(M)	8.13	4.17	1.72	1.61	1.53	1.46	3.04	
^{4}Lys(M)	7.58	3.83	1.67	1.50	1.31-1.19		1.51-1.39	2.66
^{1}Thr(m)	---	3.08	3.56	---	1.00		---	
^{2}Pro(m)	---	4.69	2.14	2.00	1.84		3.94	
^{3}Arg(m)	8.48	4.28	1.77	1.66	1.48		3.22-3.16	
^{4}Lys(m)	7.72	3.85	1.68	1.50	1.25		1.46	2.87-2.81
^{1}Thr(3)	---	4.42	3.64	---	1.02		---	
^{2}Pro(3)	---	4.85	2.36	1.79	1.53		3.47	
^{3}Arg(3)	9.65	3.88	ND	ND	ND		ND	
^{4}Lys(3)	7.40	3.68	1.64	1.60	1.24		1.44	3.69

Fig. 2. Chemical shift assignments for T1. Those in 100% DMSO at 27°C are shown. (M), (m) and (3), indicate shifts of the major, the minor and the third conformations respectively. ND indicates shift not determined.

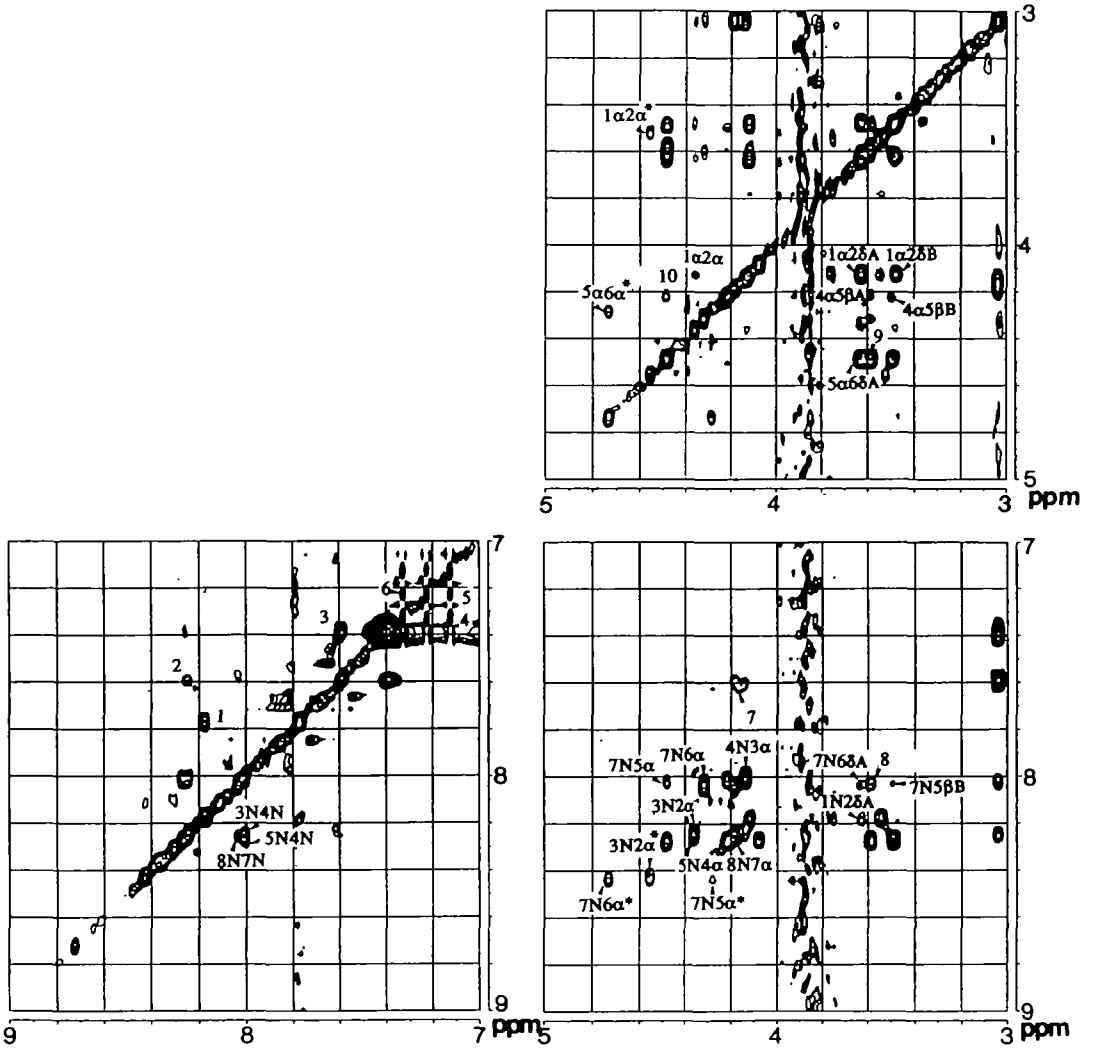

Fig. 3. Three portions of a NOESY spectrum of S2 in 90−10% DMSO/H_2O. Interresidue NOE connectivities are indicated. Those of the minor conformation are marked (*). Cross-peak [1] shows chemical exchange between NH of Ser1 and $N_\zeta H_2$ of Lys4/Lys8. Cross-peak [2] shows that between NH of Lys8 and $N\eta H$ of Arg3/Arg7. Cross-peak [3] shows that between $N\eta H$ of Arg3 and Arg7. Signals [4]−[6] arise from NH_4OH. The NOE connectivity between NH of Ser5 and $H\alpha$ of Lys4 of the minor conformation [7] is overlapped by two connectivities. NH of Arg3 to $N\epsilon H$ of Arg3 and NH of Arg7 to $N\epsilon H$ of Arg7, of the major conformation. Cross-peak [8] shows either the NOE connectivity from NH of Arg7 to $H\delta_B$ of Pro6 or that to $H\beta_A$ of Ser5 or an overlap of the two. Cross-peak [9] shows either the NOE connectivity from $H\alpha$ of Ser5 to $H\delta_B$ of Pro6 or the connectivity to $H\beta_A$ of Ser5 or an overlap of the two. Cross-peak [10] from $H\alpha$ of Lys4 to $H\alpha$ of Ser5 appears to be a spin-diffusion.

a

	NH	$C_\alpha H$	$C_\beta H$ A	$C_\beta H$ B	$C_\gamma H$ A	$C_\gamma H$ B	$C_\delta H$ A	$C_\delta H$ B	Others	
[1]Ser	8.18	4.12	3.76	3.56	---	---	---	---		
[2]Pro	---	4.36	2.09	1.72	1.84	1.84	3.63	3.48		
[3]Arg	8.22	4.14	1.64	1.46	1.48-1.42		3.04	3.04	$N_\varepsilon H$	7.62-7.56
									$N_\eta H$	7.40-7.36/6.90-6.86
[4]Lys	8.01	4.22	1.56	1.42	1.23	1.23	1.46	1.46	$C_\varepsilon H$	2.69
									$N_\zeta H$	7.76
[5]Ser	8.28	4.49	3.58	3.49	---	---	---	---		
[6]Pro	---	4.31	2.02	1.79	1.82	1.82	3.63	3.58		
[7]Arg	8.03	4.19	1.68	1.46	1.48-1.42		3.04	3.04	$N_\varepsilon H$	7.62-7.56
									$N_\eta H$	7.40-7.36/6.90-6.86
[8]Lys	8.25	4.08	1.68	1.55	1.30	1.30	1.48	1.48	$C_\varepsilon H$	2.72
									$N_\zeta H$	7.77

b

	NH	$C_\alpha H$	$C_\beta H$ A	$C_\beta H$ B	$C_\gamma H$ A	$C_\gamma H$ B	$C_\delta H$ A	$C_\delta H$ B	Others	
[1]Ser	8.23	3.52	4.18	4.18	---	---	---	---		
[2]Pro	---	4.56	2.18	1.99	1.80	1.68	3.36	3.36		
[3]Arg	8.42	4.25	1.64	1.52	1.60	1.60	2.96	2.96	$N_\varepsilon H$	8.39-8.35
									$N_\eta H$	ND
[4]Lys	8.32	4.16	1.66	1.51	1.24	1.24	ND	ND	$C_\varepsilon H$	ND
									$N_\zeta H$	ND
[5]Ser	7.63	4.28	3.48	3.40	---	---	---	---		
[6]Pro	---	4.74	2.11	1.94	1.77	1.67	3.33	3.33		
[7]Arg	8.43	4.20	1.67	1.49	1.13	1.13	3.04	3.04	$N_\varepsilon H$	7.62-7.56
									$N_\eta H$	ND
[8]Lys	8.12	4.26	1.54	1.42	1.27	1.27	ND	ND	$C_\varepsilon H$	ND
									$N_\zeta H$	ND

c

	NH	$C_\alpha H$	$C_\beta H$ A	$C_\beta H$ B	$C_\gamma H$ A	$C_\gamma H$ B	$C_\delta H$ A	$C_\delta H$ B	Others	
[1]Ser	8.16	4.18	3.78	3.58	---	---	---	---		
[2]Pro	---	4.43	2.09	1.80	1.88	1.88	3.67	3.53		
[3]Arg	8.11	4.20	1.68	1.51	1.49	1.49	3.08	3.08	$N_\varepsilon H$	7.69
									$N_\eta H$	7.76
[4]Lys	7.85	4.28	1.60	1.45	1.26	1.26	1.50	1.50	$C_\varepsilon H$	2.72
									$N_\zeta H$	8.18
[5]Ser	8.13	4.54	3.60	3.54	---	---	---	---		
[6]Pro	---	4.38	2.03	1.85	1.85	1.85	3.68	3.62		
[7]Arg	7.91	4.25	1.70	1.52	1.50	1.50	3.09	3.09	$N_\varepsilon H$	7.66
									$N_\eta H$	7.76
[8]Lys	8.08	4.14	1.72	1.58	1.34	1.34	1.54	1.54	$C_\varepsilon H$	2.75
									$N_\zeta H$	7.78

d

	NH	$C_\alpha H$	$C_\beta H$ A	$C_\beta H$ B	$C_\gamma H$ A	$C_\gamma H$ B	$C_\delta H$ A	$C_\delta H$ B	Others	
[1]Ser	8.15	3.58	ND	ND	---	---	---	---		
[2]Pro	---	4.62	2.20	2.03	1.80	1.75	3.49	3.40		
[3]Arg	8.40	4.27	1.70	1.56	1.62	1.62	3.0	3.0	$N_\varepsilon H$	8.42
									$N_\eta H$	ND
[4]Lys	7.96	4.18	1.62	1.44	1.27	ND	ND	ND	$C_\varepsilon H$	ND
									$N_\zeta H$	ND
[5]Ser	7.56	4.34	3.51	3.40	---	---	---	---		
[6]Pro	---	4.79	2.13	1.98	1.78	1.72	3.50-3.41			
[7]Arg	8.36	4.25	1.72	1.55	1.62	1.62	3.0	3.0	$N_\varepsilon H$	8.42
									$N_\eta H$	ND
[8]Lys	8.16	4.43	ND	ND	ND	ND	ND	ND	$C_\varepsilon H$	ND
									$N_\zeta H$	ND

e

	NH	$C_\alpha H$	$C_\beta H$ A	$C_\beta H$ B	$C_\gamma H$ A	$C_\gamma H$ B	$C_\delta H$ A	$C_\delta H$ B	Others	
[1]Gly	8.02	3.58	---	---	---	---	---	---		
[2]Ser	8.63	4.68	3.60	3.54	---	---	---	---		
[3]Pro	---	4.35	2.04	1.87	1.92	1.92	3.70	3.66		
[4]Lys	7.93	4.18	1.64	1.48	1.30	1.30	1.49	1.49	$C_\varepsilon H$	2.70
									$N_\zeta H$	7.76
[5]Lys	7.80	4.27	1.62	1.46	1.28	1.28	1.49	1.49	$C_\varepsilon H$	2.70
									$N_\zeta H$	7.76
[6]Ser	8.06	4.55	3.60	3.55	---	---	---	---		
[7]Pro	---	4.35	2.04	1.86	1.92	1.92	3.68	3.64		
[8]Arg	7.94	4.19	1.70	1.48	1.49	1.49	3.08	3.08	$N_\varepsilon H$	7.67
									$N_\eta H$	8.05
[9]Lys	7.77	4.13	1.69	1.50	1.29	1.29	1.53	1.53	$C_\varepsilon H$	2.75
									$N_\zeta H$	7.76
C-terminal NH_2		7.28, 7.04								

f

	NH	$C_\alpha H$	$C_\beta H$ A	$C_\beta H$ B	$C_\gamma H$ A	$C_\gamma H$ B	$C_\delta H$ A	$C_\delta H$ B	Others	
[1]Gly	ND	3.58	---	---	---	---	---	---		
[2]Ser	8.39	4.45	3.49	3.46	---	---	---	---		
[3]Pro	---	4.75	2.16	2.00	ND	ND	3.58	3.45		
[4]Lys	8.28	4.18	1.65	1.56	1.35	1.35	ND	ND	$C_\varepsilon H$	ND
									$N_\zeta H$	ND
[5]Lys	8.05	4.21	ND	ND	ND	ND	ND	ND	$C_\varepsilon H$	ND
									$N_\zeta H$	ND
[6]Ser	7.52	4.33	3.51	3.38	---	---	---	---		
[7]Pro	---	4.79	2.14	2.00	ND	ND	ND	ND		
[8]Arg	8.39	4.22	1.72	1.52	1.60	1.60	ND	ND	$N_\varepsilon H$	ND
									$N_\eta H$	ND
[9]Lys	7.98	4.16	ND	ND	ND	ND	ND	ND	$C_\varepsilon H$	ND
									$N_\zeta H$	ND
C-terminal NH_2		7.39 7.05								

Fig. 4. Chemical shift assignments for S2 and S2b of the major conformation (a) and the minor conformation (b) of S2 in a 90−10% DMSO/H_2O mixture at 4°C of the major conformation (c) and the minor conformation (d) of S2 in 100% at 27°C and of the major conformation (e) and the minor conformation (f) of S2b in 100% DMSO at 27°C. ND indicates shift not determined.

a

	T1 100% DMSO M		S2 90% DMSO I		95% DMSO I		100% DMSO I		S2b 100% DMSO I	
		m		II		II		II		II
GH_α-SNH(s)								++		
(S/T)NH-$PH_{\beta A}$	-	-	+	-	-	-	-	+	-	-
(S/T)H_α-PH_α	-	+	+	-	-	-	-	-	-	-
(S/T)H_α-$PH_{\beta B}$	-	-	-	+	-	-	-	-	-	-
(S/T)H_α-PH_γ	-	-	+	+	-	+	-	++	+	+
(S/T)H_α-$PH_{\delta A}$(s)	++	-	++	++	-	++	++	++	++	++
(S/T)H_α-$PH_{\delta B}$(s)	++	-	++	-	++	-	++	++	++	++
PH_α-(i+2)NH(s)	++	++	++	++	++	++	++	++	++	++
$PH_{\beta A}$-(i+2)NH	++	+	+	+	++	+	++	++	++	-
$PH_{\beta B}$-(i+2)NH	++	-	++	++	++	++	++	++	++	++
$PH_{\beta B}$-(i+2)H_α	-	-	-	-	-	-	-	-	+	-
PH_γ-(i+2)NH	-	-	+	+	-	-	++	++	-	-
$PH_{\delta A}$-(i+2)NH	-	-	-	+	++	-	-	++	++	++
(i+2)H_α-(i+3)NH(s)	++	++	++	++	++	++	++	++	++	++
(i+2)NH-(i+3)NH	++	+	+	++	+	+	++	ND	ND	ND
(S/T)H_α-(i+2)NH	-	-	-	+	-	+	-	+	+	++
(S/T)$H_{\beta A}$-(i+2)NH	-	-	-	-	-	++	-	++	++	-
(S/T)$H_{\beta B}$-(i+2)NH	-	-	-	++	-	-	-	++	-	-
PH_α-(i+3)NH	+	-	-	-	+	+	-	-	-	-
$PH_{\beta A}$-(i+3)NH	++	+	-	-	-	-	-	-	-	+
$PH_{\beta B}$-(i+3)NH	-	-	-	-	-	+	-	-	+	+
TH_γ-PH_α	-	+								
TH_γ-PH_δ	++	-								

b

	S2 90% DMSO	95% DMSO	100% DMSO	S2b 100% DMSO
(i+3)NH-S(i+4)NH	++	+	-	-
(i+3)H_α-S(i+4)NH(s)	++	++	++	++
(i+3)H_α-S(i+4)$H_{\beta A}$	+	-	-	-
(i+3)H_α-S(i+4)$H_{\beta B}$	+	-	-	+
(i+3)$H_{\beta A}$-S(i+4)NH	+	-	-	-
(i+3)$H_{\beta B}$-S(i+4)NH	+	-	-	-
(i+3)H_γ-S(i+4)NH	+	-	-	-
(i+3)H_δ-S(i+4)H_α	-	-	-	+

Fig. 5. Observed interresidue NOE connectivities. (a) and (b) NOE connectivities observed with the major (M) and the minor (m) components of T1. The first SP(R/K)K unit (I) and the second SP(R/K)K unit (II) of S2 and S2b are shown by + in (a). NOE connectivities between the two units of S2 and S2b are shown in (b). ++ denotes those confirmed by ROESY. Here − indicates an NOE connectivity not observed or not identified because of technical difficulty. Thus, it does not always mean that the connectivity does not exist. ND denotes an NOE connectivity not detected as the difference in chemical shift of the two proton resonances of S2b is too small. The numbers, (*i*+2), (*i*+3), etc., show those of residues counting the first Ser/Thr as the *i*-th. s denotes an NOE connectivity used for sequential assignment. The data for S2 in 95% DMSO were taken by using a 400 MHz machine (JEOL).

a

		i	i+1	i+2	i+3	i	i+1	i+2	i+3
		1	2	3	4				
T1		T	P	R	K				
		1	2	3	4	5	6	7	8
S2		S	P	R	K	S	P	R	K
	1	2	3	4	5	6	7	8	9
S2b	G	S	P	K	K	S	P	R	K

b

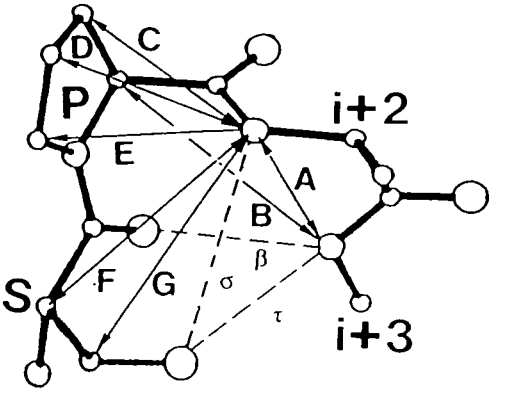

c

	T1 100% DMSO M	S2 90% DMSO I	II	S2 95% DMSO I	II	S2 100% DMSO I	II	S2b 100% DMSO I	II
(i+3) NH (i+2) NH(A)	++	+	++	+	+	++	ND	ND	ND
P H_α(B)	+	-	-	+	+	-	-	-	-
(i+2) NH P $H_{\beta A}$(C)	++	+	+	++	+	++	++	++	-
P $H_{\beta B}$(C)	++	++	++	++	++	++	++	++	++
P H_γ(D)	-	+	+	-	-	++	++	-	-
P $H_{\delta A}$(E)	-	-	+	++	-	-	++	++	++
S/T H_α(F)	-	-	+	-	+	-	+	+	++
S/T $H_{\beta A}$(G)	-	-	++	-	++	-	++	++	-
S/T $H_{\beta B}$(G)	-	-	-	-	-	-	++	-	-

Fig. 6. A turn structure adopted by the SPXX sequence. (a) The sequences of the three peptides are shown. The C-terminus of S2b is chemically blocked as $CONH_2$. (b) Lines A−G show expected NOE connectivities. A and B are expected for a β-turn, F and G, for a σ-turn and C−E for both a σ-turn and a type (I) β-turn. Possible hydrogen bonds are indicated by broken lines; σ-type (σ), τ-type (τ) and β-type (β). (c) Observed NOE connectivities coincide with turn structures selected from Figure 5.

(1984)]. The T1 peptide shows both such NOE cross-peaks (Arg3 NH−Lys4 NH, labelled 4 in Figure 1 and Pro2 H_α−Lys4 NH, labelled 8 in Figure 1). However, the Pro2 H_α−Lys4 NH cross-peak was weak and since no corresponding cross-peak was detected in ROESY, we cannot be certain that it does not arise through spin-diffusion. In S2, both SP(R/K)K units show NH(*i*+2)−NH(*i*+3) cross-peaks (Figures 3 and 5a), but not H_α(*i*+1)−NH(*i*+3) cross-peaks, while in S2b chemical shift degeneracy makes it impossible to identify the NOE interactions conclusively.

The NMR properties expected for type (I) and type (II) β-turns do not show strongly characteristic differences (Wüthrich, 1986). The two turn types differ mainly through a 180° change in the orientation of the peptide link between residues (*i*+1) and (*i*+2); a type (I) β-turn is shown in Figure 6b. An NOE connectivity would normally be expected between the (*i*+1) and (*i*+2) amide protons of a type (I) β-turn (Wüthrich *et al.*, 1984), but this cannot be observed for SP(R/K)K units since residue (*i*+1) is Pro. It might be expected that the NH of residue (*i*+2) might instead show an NOE connectivity with the H_δ protons of the Pro [shown as E in Figure 6b; Dyson *et al.* (1985)], although such an interaction might be weakened by particular puckering arrangements of the proline ring or by efficient mutual relaxation between the H_δ protons. NOE connectivities between the NH of residue (*i*+2) and either the Pro H_β signals (C in Figure 6b) or the Pro H_γ signals (D in Figure 6b) are consistent with a type (I) β-turn. For the M conformation of T1, no connectivity was observed between Arg3 NH and Pro2 H_δ, but NOE connectivities between Arg3 NH and both H_β protons of Pro2 were seen (Figure 6c), so that overall the evidence is consistent with a type (I) β-turn. The β-turn structure adopted by each SP(R/K) unit of S2 and S2b is type (I), as we observed type D

or E NOE connectivities for most of the units, together with type C observed for all the units (Figure 6c).

β-Turn formation by T1 and S2 is further supported by the temperature dependencies of their amide proton signals. In a β-turn, the amide of residue $(i+3)$ is used for hydrogen bond formation, which would be expected to lead to a temperature dependence smaller than -3 p.p.b./°C for the corresponding NH signal (Urry and Long, 1976; Iqbal and Palaram, 1982). The observed temperature dependence of the NH signal of Lys4 in T1 is extremely small (-0.7 p.p.b./°C), in marked contrast to the value found for the NH signal of Arg3 (-5.0 p.p.b./°C) and these values are preserved over a wide range of concentrations (0.5–5 mg/ml).

The observed temperature dependence of the amide proton resonances of S2 in 100% DMSO are Arg3, -1.7 p.p.b./°C, Lys4, -2.3 p.p.b./°C, Ser5, -2.8 p.p.b./°C, Arg7, -1.7 p.p.b./°C and Lys8, -1.5 p.p.b./°C. The value for Ser5 is the largest, but the others seem likely to be protected to some extent from the solvent. This suggests some involvement of both the $(i+2)$ and $(i+3)$ amides in hydrogen bonding. In fact, approximately 18% of the SPXX fragments in protein crystal structures have a hydrogen bond between the amide of residue $(i+2)$ and the serine hydroxyl oxygen. The resulting structure is called a σ-turn (Suzuki and Yagi, 1991) and when combined with a type (I) β-turn it is called a $\beta\sigma$-turn, a turn with two hydrogen bonds (Figure 6b). A σ-turn is not compatible with a type (II) β-turn but with a type (I) β-turn.

Based on the coordinates given in Suzuki and Yagi (1991), a σ-turn would be predicted to show NOE connectivities between the NH of residue $(i+2)$ and the H_α and H_β protons of Ser(i) (shown as F and G respectively in Figure 6b). Thus, of the various connectivities shown in Figure 6b, A and B are expected for a β-turn of any type, F and G are expected for a σ-turn and C, D and E are expected for either a σ-turn or a type (I) β-turn. On this basis, the two SP(R/K)K units in S2 and S2b show NOE characteristics of both turn structure types (Figure 6c), which is also consistent with the temperature dependence measurements. However, it is not possible to say whether the structure adopted by the SP(R/K)K units is a 'static' $\beta\sigma$-turn or a dynamic interconversion of β- and σ-turns.

In contrast to the cases of S2 and S2b, no NOE connectivities characteristic of a σ-turn were observed for peptide T1 (Figure 6c). Moreover, the large temperature dependence of the NH signal of Arg3 suggests that this amide is not involved in hydrogen bond formation. This is again consistent with the statistical study of Suzuki and Yagi (1991); more than 70% of type (I) β-turns in TPXX sequences in protein crystal structures have a second hydrogen bond between the side chain oxygen of Thr and the NH proton of residue $(i+3)$, resulting in what is called a τ-type β-turn. In this structure, the NH of residue $(i+2)$ is not involved in hydrogen bond formation, while that of residue $(i+3)$ is expected to be strongly shielded from the solvent through participation in a bifurcated hydrogen bond [Figure 6b, and see also Figure 1 of Suzuki and Yagi (1991)]. The extremely small temperature dependence of the NH proton of Lys4 suggests that peptide T1 may well adopt a $\beta\tau$-turn conformation. As has been discussed by Suzuki and Yagi (1991) slight differences between the turn structures adopted by the TP and SP sequences are probably caused by the methyl group of Thr, which prevents the side chain from locating deeply inside the turn.

Conformational energy calculations for the T1 peptide in the gas phase have been reported by Anderson and Scheraga (1978), in which the lowest energy conformation found was a γ-turn structure formed by the Pro–Arg sequence, with an additional hydrogen bond from the OH of Thr1 to the CO of Lys4; this structure is incompatible with our observations. A weak NOE connectivity between Pro2 H_β and Lys4 NH was also observed in the spectra of T1 (Figure 5a). This might arise in the extended structure, given that the corresponding distance is approximately 4 Å in a type (I) β-turn.

Minor conformation of T1

In the m conformation, the main chain NH of Lys may also be involved in hydrogen bond formation; the temperature dependences of the Arg and Lys amides are -3.6 p.p.b./°C and -1.2 p.p.b./°C respectively. The Pro–Arg–Lys connection in the m conformation seems to resemble that in the M conformer (compare NOE connectivities shown in Figure 5a). However, the CO of Thr cannot be the acceptor in any hydrogen bond made by the NH of Lys, since the *cis* peptide bond between Thr and Pro causes this carbonyl to project away from the Lys NH proton. A possible alternative hydrogen bond acceptor is the side chain oxygen of Thr. If the Thr residue is rotated through 180° around the peptide bond between Thr and Pro, the side chain oxygen of Thr can approach the NH proton of Lys. Observed NOE connectivities in the m conformation, between Thr CH_3 and Pro H_α, can be explained by such a structure. The populations of the m conformations of S2 and S2b are too small to allow discussion of their structures.

Connectivity between the two units

The connection between the two SP(R/K)K units has rotational freedom, because not many NOE connectivities were observed between the two units (Figure 5b). However, for S2 in 90% DMSO at 4°C, together with the other NOE connectivities between Lys4 and Ser5, an NOE connectivity between the amides on Lys4 and Ser5 was observed (Figure 5b). This suggests that the sequence, PRKS, also folds into a β-turn. Thus, the N-terminal five residues of S2, SPRKS, seems to fold into a short 3_{10} helix. The second SPRK unit also folds into a β-turn. In other words the structured state of S2 in this environment is described as a 3_{10} helix broken at the second Pro, which lacks an amide proton to continue the helix (Figure 7a). The broken 3_{10} helical structure of S2 is actually very close to a structure proposed for S2 (Suzuki, 1989), in which the second unit is rotated relative to the first, breaking the hydrogen bond between the two units [compare Figure 7b of this paper with Figure 6b in Suzuki (1989)].

Structure of the motif in the complex with DNA

In a previous paper (Suzuki, 1989) a model based on a β-turn, the '1989 model', was used for a model building study of the S2–DNA complex. However, the present results show that a turn structure adopted by the SPKK motif may well be a dynamic conversion of a β-turn and a σ-turn, so that a σ-turn is another possibility for the structure used to bind to DNA. So it seems relevant to investigate models of the S2–DNA complex in which the SPKK motif adopts a σ-turn. In this study it is assumed that two basic side chains of the SPKK motif bind to phosphates of DNA.

If folded into β-turns, two repeats of the SPKK motif can cover two bases (Suzuki, 1989). The SPKK motif binds to the minor groove at A–T-rich sequences and its DNA-binding mode is competitive with that of a dye, Hoechst 33258 (Churchill and Suzuki, 1989; Suzuki, 1989). The Ser amides in the 1989 model can be superimposed well onto the amides of netropsin, another ligand similar to Hoechst 33258 in DNA binding (Suzuki, 1989).

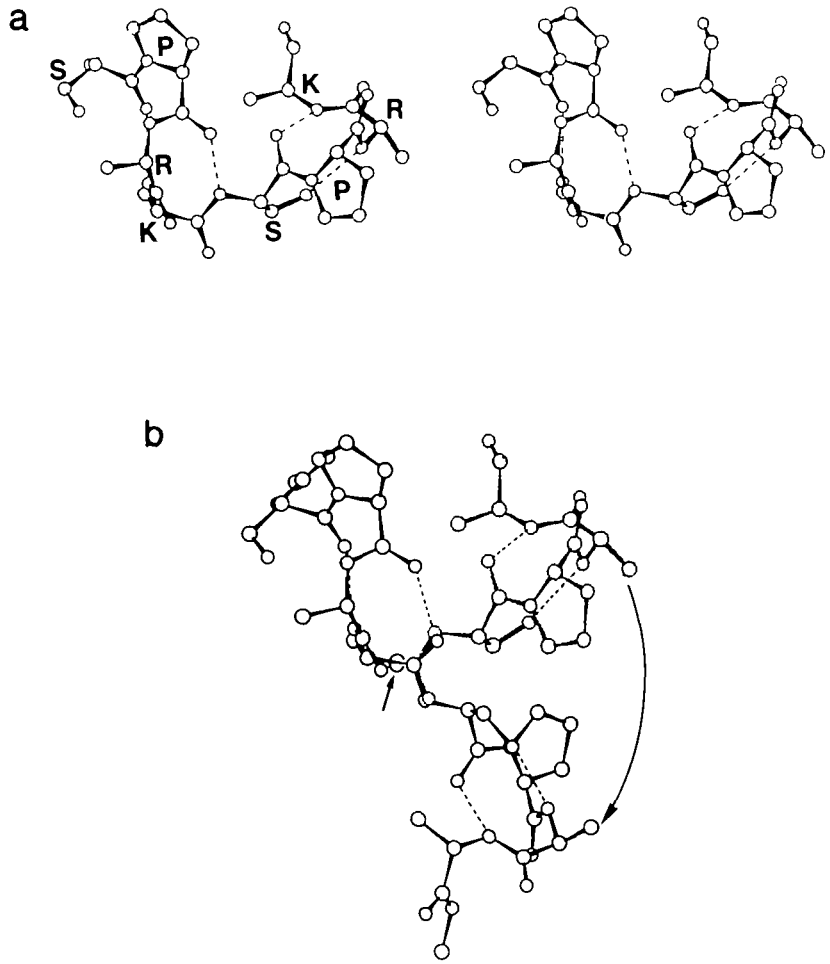

Fig. 7. NMR structure of S2. (a) A stereo view of a structure proposed for the major conformation of S2 in 9:1 DMSO−H_2O mixture, based on the NMR analysis, is shown. The dihedral angles chosen are Ser1 (X, −140), Pro2 (−60, −30), Lys3 (−60, −30), Lys4 (−60, −30), Ser5 (−178, 140), Pro6 (−60, −30), Arg7 (−90, −0) and Lys8 (60, X). The Ser−Pro peptide links are *trans*. For clarity, the side chain beyond C_β is omitted for Arg and Lys. The $\chi 1$ angle chosen for two Ser is 140°. The proposed hydrogen bonds are indicated by broken lines. (b) The ψ angle of Lys3 (marked with a circle) is rotated to 159° so that the hydrogen bond from Ser5 NH to Lys4 CO is broken.

These amides of netropsin are found in a crystal to bind directly to the A−T bases of DNA in the minor groove (Kopka *et al.*, 1985). However, if the two SPKK repeats in this model are superimposed onto a netropsin molecule in the minor groove of DNA and if the structure of the DNA is not changed at all, a few awkward conflicts occur between the S2 molecule and the DNA, because the 1989 model for S2 is more bulky than netropsin. If the Ser amide is to penetrate deeply into the minor groove, the side chain of the preceding Lys would also lie very deep inside the minor groove and its long side chain would have steric conflicts with the phosphate helices of DNA.

If the SPKK motif is folded into a σ-turn rather than a β-turn, the distance between the two Ser amides in S2 increases (Figure 8a). One SPKK motif can cover two base pairs of DNA and the two amides can be superimposed onto first and third amides of netropsin (Figure 8b) instead of onto the first and second amides as was the case with the 1989 model. The new model is much flatter and might therefore be expected to be a better one to fit into the minor groove, but in fact detailed model building shows otherwise. If the SPKK motif is folded into a σ-turn and if a repeat of such structures is placed very deep inside the minor groove so that Ser residues can hydrogen bond to A−T base pairs directly, the side chains of the two basic residues preceding the Ser have strong steric clashes with the sugar-phosphate backbone of the DNA (Figure 8d).

A more plausible model for binding can be constructed by moving the SPKK motif further into the solvent so that it does not penetrate so deeply into the minor groove. In this position there are not many steric clashes and it is possible for the two basic side chains to interact favourably with the negatively charged phosphate groups (Figure 8e). Furthermore, as shown in Figure 8f, even in this 'less penetrating' form of attachment, there is still tight packing between parts of the SPKK motif and the DNA minor groove. Formation of direct hydrogen bonds between the amides of the SPKK repeats and the DNA bases does not appear to be possible. Consequently, the close correspondence between amides of the netropsin structure and those of the SPKK motif might reflect the fact that both span two base pairs. If this is the case, the A−T preference of the SPKK motif arises not from direct recognition of A−T base pairs by the amides but from recognition of other structural characteristics, such as the narrow minor groove of A−T-rich DNA

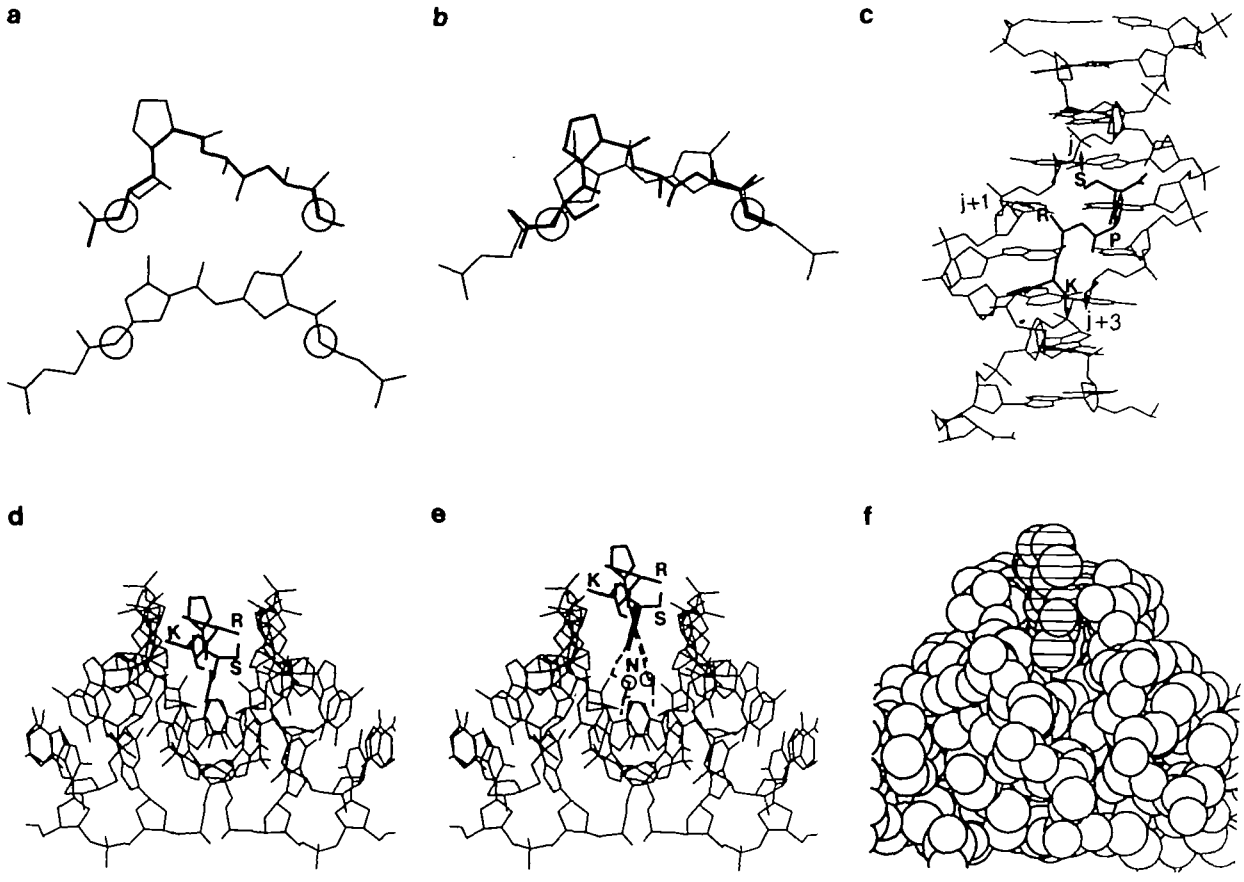

Fig. 8. A model for the DNA–SPKK complex. (**a**) and (**b**) A σ-turn adopted by the SPKK motif (*top*) is compared with netropsin (bottom). A model of the SPKK motif of the sequence, Ser–Pro–Arg–Lys, is built using dihedral angles; Ser1 (120, −150), Pro2 (−60, −20), Arg3 (−60, 120) and Lys4 (−120, 120). Only C_β atoms are drawn for the side chains of R and K. Amides of the two molecules superimposed onto each other in (**b**) are marked with circles. (**c**) A side view of the model in (**e**) and (**f**) is shown. The SPRK peptide bridges the two phosphate strands of DNA across the minor groove. In this model the Ser hydroxyl and the Arg side chain interact with the phosphates on the A-strand, denoted (j) and ($j+1$) respectively, while the Lys side chain interacts with phosphate ($j+3$) on the B-strand (see text). (**d**) To make a model for the complex of the SPKK motif and DNA, a σ-turn adopted by the SPKK motif is superimposed onto netropsin in the crystal structure of DNA–netropsin complex and then the netropsin molecule is deleted. In this structure the SPRK peptide lies deep inside the minor groove. Steric clashes with the backbone phosphates are unavoidable. (**e**) The SPRK peptide in (**d**) is moved outwards from the minor groove so that the two basic side chains can extend over the minor groove of DNA. The netropsin molecule (N) is also shown to compare the locations of the two molecules. The two amides of netropsin which are overlapped onto those of S2 in (**b**) are circled. (**f**) A van der Waals display of the model in (**e**) is shown. The peptide is hatched. DNA and the peptide pack tightly together.

(Churchill and Suzuki, 1989). Even so, comparison of a peptide structure with a ligand of Hoechst type, which was first described in the 1989 paper (Suzuki, 1989), is still useful to understand the number of bases covered by the peptide. Indirect hydrogen bonds between the peptides and DNA through water molecules might be still possible; such hydrogen bonds might provide another way of explaining the overlap of the amides of the two molecules.

One can also argue that in binding to the SPKK motif, the DNA changes its structure significantly from that observed in the netropsin–DNA complex. This change in structure could result in a widening of the minor groove that would allow the SPKK amides to penetrate more deeply. However, it is hard to judge the extent to which DNA can alter its conformation and it was felt best to base our model on established geometry.

We are collaborating with the group of Dr Molinali in Milano to determine the solution structure of a complex of DNA and G[SP(R/K)(R/K)]$_4$. When the peptide is mixed with an oligo-DNA, its chemical shifts are changed, although the peptide still seems to be extended to some extent (Molinari *et al.*, unpublished). The chemical shifts of the DNA protons are not much changed. So far we have not succeeded in detecting NOE connectivities between the peptide and DNA. This might not be surprising, as there are no proton (DNA)–proton (peptide) distances less than 5 Å in the model shown in Figure 8e.

Comparison with other models and a structure

It might be of some relevance to compare the model discussed in this paper with other models and the structure of a DNA-binding protein. The crystal structure of the complex of the DNA-binding domain of Gal4 and its cognate DNA has been solved (Marmorstein *et al.*, 1992). The DNA-binding domain of Gal4 is composed of three parts, a C6 class Zn finger, a dimerization domain and a linker connecting the other two domains. The linker sequence, SPKTKRSPLTR, is a variant of the SPKK repeat and contains two SPXX sequences. The two sequences are not typical for the SPKK motif, nor are the two SPXX sequences adjacent. Nevertheless, the linker adopts a structure similar to the 1989 model or the model discussed in this paper and it binds to the minor groove and bridges the two phosphate strands. The second SPXX sequence in the linker folds into a sharp turn, while the first sequence adopts a more extended conformation.

After the 1989 model (Suzuki, 1989) had been published, Reeves and Nissen (1990) proposed a model for DNA binding of the TPKRPRGRPKG sequence of the HMG I protein. In their model the TPKR sequence folds into a kind of Asx-turn, while the rest adopts an extended conformation. Three of the main chain amides bind to DNA directly. However, there are some difficulties with this model. As indicated previously, if the main chain amides penetrate deeply into the minor groove to make hydrogen bonds, steric clashes involving the basic side chains are inevitable. Also, the N-terminal proline appears to adopt an improbable *cis* conformation without any apparent structural reason. A β-turn type model such as the 1989 model might be more appropriate for the motif starting with Thr than for that with Ser, as the T1 peptide in solution does not show the characteristics of a σ-turn. Although a simple secondary structure prediction suggests β-turn formation by the SPKK repeat (Poccia, 1987), formation of the σ type hydrogen bond might be essential to the sequences with Ser.

The σ-turn type model for DNA binding of S2 resembles the model for DNA binding of poly Arg proposed approximately 40 years ago (Feughelman *et al.*, 1955). In our new model, however, not all DNA phosphates are bound by basic side chains, as one SPKK unit covers two base pairs with four phosphates. It is likely that the Ser hydroxyl also interacts with a phosphate. Denoting this position on the DNA by (j) and on the peptide by (i), Figure 8c shows that Arg ($i+2$) interacts with phosphate ($j+1$) and Lys ($i+3$) interacts with the phosphate ($j+3$) on the other phosphate strand. Phosphate ($j+1$) might also interact with the proline carbonyl ($i+1$). It is most likely a turn structure adopted by the Ser−Pro sequence is used to change the direction of the main chain of the peptide allowing it to follow the minor groove of DNA. This feature resembles that of the pentapeptide model proposed by von Holt *et al.* (1984). Based on the curvature of the Ser−Pro connection (Figure 8a), it is likely that Pro is placed further outside the DNA into the solvent than is the Ser so that the curvature of the peptide fits the direction of the major groove of DNA. Also, the Ser−Pro sequence may be important for regulating DNA-binding ability of the motif by phosphorylation (Suzuki *et al.*, 1990). Further study is necessary to conclude which model, the 1989 model or the model discussed in this paper, is closer to the truth.

Acknowledgements

We thank Dr D.Neuhaus for his help with NMR measurements, reading of the manuscript and helpful discussion. We thank Professor A.Klug and Dr J.Finch for their reading of the manuscript and helpful discussion and Ms H.Kajiura (National Institute for Basic Biology), Mr T.Yamazaki and Dr K.Nagayama (JEOL), for their help in measuring NMR spectra during the early stages of the work in Japan. M.G. acknowledges a Herchel-Smith fellowship for support.

References

Anderson,J.S. and Sheraga,H.A. (1978) *Macromolecules*, **11**, 812−819.
Bernstein,F.C., Koetzle,T.F., Williams,G.J.B., Meyer,E.F.,Jr, Brice,M.D., Rodgers,J.R., Kennard,O., Shimanouchi,T. and Tasumi,M. (1977) *J. Mol. Biol.*, **112**, 535−542.
Bodenhausen,G., Vold,R.I. and Vold,R.R. (1980) *J. Magnet. Res.*, **37**, 93−106.
Brooks,B.R., Bruccoleri,R.E., Olafson,B.D., States,D.J., Swaminathan,S. and Karplus,M. (1983) *J. Comput. Chem.*, **4**, 187−217.
Brunger,A.T., Kuriyan,J. and Karplus,M. (1987) *Science*, **235**, 458−460.
Churchill,M.E.A. and Suzuki,M. (1989) *EMBO J.*, **8**, 4189−4195.
Dayringer,H.E., Tramontano,A., Sprang,S.R. and Fletterick,R.J. (1986) *J. Mol. Graph.*, **4**, 82−87.
Dyson,H.J., Cross,K.J., Houghten,R.A., Wilson,I.A., Wright,P.E. and Lerner,R.A. (1985) *Nature*, **318**, 480−483.
Erard,M., Lakhdra-Ghazal,F. and Amalric,F. (1990) *Eur. J. Biochem.*, **191**, 19−26.
Feughelman,M., Langridge,R., Seeds,W.R., Stokes,A.R., Wilson,H.R., Hooper,C.W., Wilkins,M.H.A., Barclay,R.K. and Hamilton,L.Q. (1955) *Nature*, **175**, 834−838.
Iqbal,M. and Palaram,P. (1982) *Biopolymers*, **21**, 1427−1433.
Jones,T.A. (1982) In Sayre,D. (ed.), *Computational Crystallography*. Clarendon Press, Oxford, pp. 303−317.
Kent,H.A. (1975) *J. Biol. Reproduct.*, **12**, 504−507.
Kopka,M.L., Yoon,C., Goodsell,D., Pjura,P. and Dickerson,R.E. (1985) *J. Mol. Biol.*, **183**, 553−565.
Lapeyer,B., Bourlion,H. and Amalric,F. (1987) *Proc. Natl Acad. Sci. USA*, **84**, 1472−1476.
Lesk,A.M. and Hardmann,K.D. (1982) *Science*, **216**, 539−540.
Lund,T., Dahl,H.D., Mork,E., Holtlund,L. and Laland,S.G. (1987) *Biochem. Biophys. Res. Commun.*, **146**, 725−730.
Marion,D. and Wüthrich,K. (1983) *Biochem. Biophys. Res. Commun.*, **113**, 967−974.
Marmorstein,R., Carey,M., Ptashne,M. and Harrison,S.C. (1992) *Nature*, **356**, 408−414.
Poccia,D. (1987) In Schlegel,R.A. and Halleck,M.S. (eds), *Molecular Recognition of Nuclear Event in Mitosis and Meiosis*. Academic Press, Orlando, pp. 149−178.
Rance,M. (1987) *J. Magnet. Res.*, **74**, 557−564.
Reeves,R. and Nissen,M.S. (1990) *J. Biol. Chem.*, **265**, 8573−8582.
Shaka,A.J., Lee,C.J. and Pines,A. (1988) *J. Magnet. Res.*, **77**, 274−293.
Suzuki,M. (1989) *EMBO J.*, **8**, 797−804.
Suzuki,M. (1991) In Eckstein,F. and Lilley,D.M.J. (eds), *Nucleic Acids and Molecular Biology*. Springer-Verlag, Berlin-Heidelberg, pp. 126−140.
Suzuki,M. and Yagi,N. (1991) *Proc. R. Soc. Lond. B.*, **246**, 231−235.
Suzuki,M., Sohma,H., Yazawa,M., Yagi,K. and Ebashi,S. (1990) *J. Biochem.*, **108**, 356−364.
Urry,D.W. and Long,M.M. (1976) *CRC Crit. Rev. Biochem.*, **4**, 1−45.
von Holt,C., de Groot,P., Schwager,S. and Brandt,W.F. (1984) In Stein,G.S., Stein,J.L. and Marzluff,W.F. (eds), *Histone Genes*. Wiley-Interscience, New York, pp. 65−105.
Wüthrich,K. (1976) *NMR in Biological Research: Peptides and Proteins*. North-Holland Publishing, Amsterdam.
Wüthrich,K. (1986) *NMR of Proteins and Nucleic Acids*. John Wiley, New York.
Wüthrich,K., Billeter,M. and Brown,W. (1984) *J. Mol. Biol.*, **180**, 741−756.
Zuiderweg,E.R.P., Hallenga,K. and Olejniczak,E.T. (1986) *J. Magnet. Res.*, **70**, 336−343.

Received on December 2, 1992; revised on March 1, 1993; accepted on April 19, 1993